



DIGITAL ACCESS TO SCHOLARSHIP AT HARVARD

In vitro evaluation of bi-layer silk fibroin scaffolds for gastrointestinal tissue engineering

The Harvard community has made this article openly available.
[Please share](#) how this access benefits you. Your story matters.

Citation	Franck, Debra, Yeun Goo Chung, Jeannine Coburn, David L Kaplan, Carlos R Estrada, and Joshua R Mauney. 2014. "In vitro evaluation of bi-layer silk fibroin scaffolds for gastrointestinal tissue engineering." <i>Journal of Tissue Engineering</i> 5 (1): 2041731414556849. doi:10.1177/2041731414556849. http://dx.doi.org/10.1177/2041731414556849 .
Published Version	doi:10.1177/2041731414556849
Accessed	February 17, 2015 6:16:35 AM EST
Citable Link	http://nrs.harvard.edu/urn-3:HUL.InstRepos:13454748
Terms of Use	This article was downloaded from Harvard University's DASH repository, and is made available under the terms and conditions applicable to Other Posted Material, as set forth at http://nrs.harvard.edu/urn-3:HUL.InstRepos:dash.current.terms-of-use#LAA

(Article begins on next page)

In vitro evaluation of bi-layer silk fibroin scaffolds for gastrointestinal tissue engineering

Debra Franck¹, Yeun Goo Chung^{1,2}, Jeannine Coburn³, David L Kaplan³, Carlos R Estrada Jr^{1,2} and Joshua R Mauney^{1,2}

Abstract

Silk fibroin scaffolds were investigated for their ability to support attachment, proliferation, and differentiation of human gastrointestinal epithelial and smooth muscle cell lines in order to ascertain their potential for tissue engineering. A bi-layer silk fibroin matrix composed of a porous silk fibroin foam annealed to a homogeneous silk fibroin film was evaluated in parallel with small intestinal submucosa scaffolds. AlamarBlue analysis revealed that silk fibroin scaffolds supported significantly higher levels of small intestinal smooth muscle cell, colon smooth muscle cell, and esophageal smooth muscle cell attachment in comparison to small intestinal submucosa. Following 7 days of culture, relative numbers of each smooth muscle cell population maintained on both scaffold groups were significantly elevated over respective 1-day levels—indicative of cell proliferation. Real-time reverse transcription polymerase chain reaction and immunohistochemical analyses demonstrated that both silk fibroin and small intestinal submucosa scaffolds were permissive for contractile differentiation of small intestinal smooth muscle cell, colon smooth muscle cell, esophageal smooth muscle cell as determined by significant upregulation of α -smooth muscle actin and SM22 α messenger RNA and protein expression levels following transforming growth factor- β 1 stimulation. AlamarBlue analysis demonstrated that both matrix groups supported similar degrees of attachment and proliferation of gastrointestinal epithelial cell lines including colonic T84 cells and esophageal epithelial cells. Following 14 days of culture on both matrices, spontaneous differentiation of T84 cells toward an enterocyte lineage was confirmed by expression of brush border enzymes, lactase, and maltase, as determined by real-time reverse transcription polymerase chain reaction and immunohistochemical analyses. In contrast to small intestinal submucosa scaffolds, silk fibroin scaffolds supported spontaneous differentiation of esophageal epithelial cells toward a suprabasal cell lineage as indicated by significant upregulation of cytokeratin 4 and cytokeratin 13 messenger RNA transcript levels. In addition, esophageal epithelial cells maintained on silk fibroin scaffolds also produced significantly higher involucrin messenger RNA transcript levels in comparison to small intestinal submucosa counterparts, indicating an increased propensity for superficial, squamous cell specification. Collectively, these data provide evidence for the potential of silk fibroin scaffolds for gastrointestinal tissue engineering applications.

Keywords

Colon, esophagus, small intestine, silk fibroin, tissue engineering

Received: 26 August 2014; accepted: 25 September 2014

¹Urological Diseases Research Center, Department of Urology, Boston Children's Hospital, Boston, MA, USA.

²Department of Surgery, Harvard Medical School, Boston, MA, USA.

³Department of Biomedical Engineering, Tufts University, Medford, MA, USA.

Corresponding authors:

Joshua R Mauney, Urological Diseases Research Center, Department of Urology, Boston Children's Hospital, John F. Enders Research

Laboratories, 300 Longwood Ave., Rm. 1009, Boston, MA 02115, USA.

Email: joshua.mauney@childrens.harvard.edu

Carlos R Estrada Jr, Department of Urology, Boston Children's Hospital, 300 Longwood Ave., Hunnewell 3, Boston, MA 02115, USA.

Email: carlos.estrada@childrens.harvard.edu



Introduction

The gastrointestinal (GI) tract is a continuous system of tubular organs, including the esophagus, stomach, small intestine, and colon, which is responsible for the transport and digestion of food, absorption of nutrients, and excretion of waste. A wide spectrum of benign and malignant GI pathologies frequently requires surgical intervention to repair or replace damaged tissues in order to preserve alimentary function. In patients afflicted with short bowel syndrome (SBS) wherein a reduction of more than 70% of normal jejunal–ileal length has occurred,¹ intestinal lengthening procedures² and allogeneic intestinal transplantation³ have been deployed to increase functional absorptive capacity. However, major drawbacks with these approaches exist, including the continued reliance on total parenteral nutrition following intestinal elongation^{4,5} as well as immunorejection risks in individuals receiving allografts.^{6,7} Long-gap esophageal defects resulting from esophageal atresia, strictures, and squamous cell carcinoma are often repaired with gastric pull-up or interposition grafts using either jejunum or colon.^{8,9} Unfortunately, these methods are associated with substantial reductions in esophageal motility as well as donor site morbidity^{10,11} which can severely impair patient quality of life.^{12,13} Surgical colon resection is frequently utilized for management of disorders of the large intestine such as Crohn's and Hirschsprung's diseases.¹⁴ However, increased stool frequency and fecal incontinence represent undesirable consequences of this mode of therapy.^{15,16} Given the limitations associated with conventional surgical approaches, there exists a substantial need for the development of alternative strategies for GI reconstruction.

Tissue engineering strategies deploying three-dimensional (3D) biodegradable scaffolds either alone or seeded with primary or multi-potent cell sources have been investigated as implants for GI defect repair.^{17–19} Cell-free grafts composed of decellularized tissues such as small intestinal submucosa (SIS), acellular dermis, collagen-based sponges, and gastric acellular matrices have been shown to promote de novo epithelial and smooth muscle tissue formation in animal models of esophageal and small intestinal injury by supporting host tissue integration.^{18,20–22} However, deleterious side effects including graft contracture, implant perforation, obstruction, and stenosis are frequently observed,^{23–26} thus raising concerns over the translational potential of these biomaterial configurations. Synthetic polyester-based matrices seeded with organoid units, multi-cellular clusters of epithelium, and mesenchyme harvested from neonatal or postnatal GI tissue have been reported to encourage tissue regeneration in defects of the esophagus,²⁷ small intestine,²⁸ and colon.²⁹ Unfortunately, degradation metabolites of polyesters are known to elicit chronic inflammatory responses in vivo³⁰ and therefore have the potential to negatively impact long-term organ function due to adverse foreign

body reactions.³¹ In addition, the limited availability of human neonatal or postnatal donor tissue for organoid procurement represents a practical barrier for widespread clinical utilization of this technology.³²

We hypothesize that the ideal strategy for GI tissue reconstruction would consist of an “off-the-shelf” acellular implant with the structural, mechanical, and degradative properties necessary to provide initial reinforcement to defect sites while allowing for gradual remodeling, host tissue ingrowth, and subsequent maturation of site-appropriate, functional tissue in the absence of adverse inflammatory reactions. Biomaterials derived from *Bombyx mori* silk fibroin (SF) represent attractive candidates for GI tissue engineering due to their high structural strength and elasticity,³³ diverse processing plasticity,³⁴ tunable biodegradability,^{35,36} and low immunogenicity.^{31,33} Previous studies from our laboratory have demonstrated the feasibility of bi-layer SF scaffolds to serve as acellular, biodegradable matrices for functional tissue regeneration of bladder^{37–39} and urethral⁴⁰ defects. The unique architecture of the bi-layer SF scaffold configuration is also particularly suited for repair of GI perforations or replacement of diseased tissue sites since its porous compartment has the potential to promote ingrowth of surrounding host tissue while an SF film annealed to the porous layer is designed to provide a fluid-tight seal for retention of GI contents during defect consolidation.^{37,38} In the present study, we investigated the biocompatibility of this scaffold design for GI tissue engineering by evaluating its ability to support attachment, proliferation, and differentiation of human GI epithelial and smooth muscle cell (SMC) lines in vitro. The ability of biomaterials to support these cellular processes is crucial for promoting host tissue integration and functional maturation of regenerating tissue.

Materials and methods

Biomaterials

Bi-layer SF scaffolds were prepared using previously described procedures.^{37,40,41} Briefly, cocoons from *Bombyx mori* were boiled for 20 min in an aqueous solution of 0.02 M Na₂CO₃, and rinsed with distilled water to eliminate sericin and other contaminating proteins. Purified SF was solubilized in a 9 M LiBr solution and dialyzed (Pierce, Woburn, MA) against distilled water for 4 days with volume changes every 8 h. The resultant aqueous SF solution was diluted with distilled water to 6%–8% wt/vol and utilized for scaffold fabrication. The SF solution (8% wt/vol) was poured into a rectangular casting vessel and dried in a laminar flow hood at room temperature for 48 h to achieve formation of a SF film. A 6% wt/vol SF solution was then mixed with sieved granular NaCl (500–600 μM, average crystal size) in a ratio of 2 g NaCl per mL of SF solution and layered on to the surface of the SF film. The

resultant solution was allowed to cast and fuse to the SF film for 48 h at 37°C, and NaCl was subsequently removed by washing the scaffold for 72 h in distilled water with regular volume changes. The morphology of the bi-layer SF scaffold has been previously reported.³⁷ Briefly, the solvent-cast/NaCl-leached layer comprised the bulk of the total matrix thickness (2 mm) and resembled a foam configuration with large pores (pore size, ~400 µm) interconnected by a network of smaller pores dispersed along their periphery. This compartment was buttressed on the external face with a homogeneous, non-porous SF layer (200 µm thick) generated by film annealment during casting. Prior to in vitro experiments, bi-layer SF scaffolds were sterilized in 70% ethanol and rinsed in phosphate buffered saline (PBS) overnight. SIS matrices (Cook, Bloomington, IN) were evaluated in parallel as a standard point of comparison. Tensile properties of both scaffold configurations have been previously reported.³⁷

GI SMCs

Primary SMC (passage 1) derived from human small intestine SMC (siSMC), colon SMC (cSMC), and esophageal SMC (eSMC) (ScienCell Research Laboratories, Carlsbad, CA) were expanded for two additional passages on tissue culture plastic in SMC medium (SMCM, ScienCell) according to the manufacturer's instructions. SMCM consists of a bicarbonate buffered basal medium containing 2% fetal bovine serum (FBS), 1% of SMC growth supplement (SMCGS), and 1% of penicillin/streptomycin solution (P/S). For cell attachment and proliferation analyses, SMC lines (passage 4) were independently seeded on bi-layer SF and SIS matrices (10⁶ cells/scaffold) in SMCM and cultured statically in conical tubes for up to 7 days. Medium exchange was carried out every 3 days. To induce contractile differentiation, SMC lines were seeded on matrices as described above, serum depleted for 24 h in SMCM containing 0.5% fetal calf serum (FCS), and subsequently exposed to 2.5 ng/mL transforming growth factor-β1 (TGF-β1) (R&D Systems, Minneapolis, MN) for 24 h. Control cultures were maintained in parallel in SMCM for 3 days.

GI epithelial cells

The human T84 epithelial cell line derived from colonic adenocarcinoma (American Type Culture Collection (ATCC), Manassas, VA) was expanded to passage 56 on tissue culture plastic in complete growth medium consisting of a 1:1 mixture of Ham's F12 medium and Dulbecco's modified Eagle's medium (DMEM), 2.5 mM L-glutamine, 15 mM hydroxyethyl piperazine ethanesulfonic acid (HEPES), 0.5 mM sodium pyruvate, and 1200 mg/L sodium bicarbonate (DMEM:F-12, ATCC), supplemented with 5% FBS (Life Technologies, Grand Island, NY). Human primary esophageal epithelial (eEP) cells (passage

1) (ScienCell) were expanded for three additional passages on tissue culture plastic in Epithelial Cell Medium-2 (EpiCM-2, ScienCell) according to the manufacturer's instructions. EpiCM-2 consists of 1% of epithelial cell growth supplement-2 (EpiCGS-2) and 1% of P/S. eEP and T84 cells were independently seeded on bi-layer SF and SIS matrices (10⁶ cells/scaffold) and cultured statically in conical tubes in respective growth media for up to 7 or 14 days to assess cell attachment, extent of proliferation, and differentiation status. Medium exchange was performed every 3 days.

Cell attachment and proliferation analyses

The relative number of metabolically active cells following 24 h of cell seeding and over the course of cultivation on each matrix group was determined by the alamarBlue assay (Life Technologies) according to the manufacturer's instructions. Briefly, scaffolds seeded with cell lines were incubated in their respective culture medium supplemented with 10% alamarBlue reagent for 2 h at 37°C with 5% CO₂. Post reaction medium aliquots (100 µL) were transferred to 96-well plates and quantified for fluorescence intensity within a FLUOstar Omega plate reader (BMG Labtech Inc., Durham, NC) using an excitation wavelength of 560 nm and an emission wavelength of 590 nm. Non-seeded matrices were screened in parallel as background controls. Relative cell numbers were calculated as the degree of relative fluorescence units (FU) per construct as previously described.⁴²

Messenger RNA analysis

Total RNA was extracted from cell seeded scaffolds according to the single step acid-phenol guanidinium method⁴³ using Trizol reagent (Life Technologies). Messenger RNA (mRNA) was enriched from total RNA using the RNeasy kit (Qiagen Inc., Valencia, CA), and complementary DNAs (cDNAs) were synthesized using the High-Capacity cDNA Transcription kit (Applied Biosystems, Foster City, CA) following the manufacturer's instructions. Real-time reverse transcription polymerase chain reaction (RT-PCR) reactions were performed and analyzed using the Applied Biosystems StepOnePlus™ Real-time PCR Detection System and StepOne Software (version 2.1). cDNA samples were assessed for genes of interest and the housekeeping gene, GAPDH, in independent reactions using the Taqman Universal PCR master mix in combination with commercially available primers and probes consisting of Assays-on-Demand™ Gene Expression kits (Applied Biosystems) following the manufacturer's instructions. Expression kits included α-smooth muscle actin (SMA), Hs00426835_g1; SM22α, Hs00162558_m1; lactase, Hs00158722_m1; maltase, Hs01090216_m1; cytokeratin (CK) 4, Hs00361611_m1; CK13, Hs00357961_g1;

involucrin, Hs00846307_s1; GAPDH, Hs02758991_g1. For each cDNA sample, the threshold cycle (Ct) was defined as the cycle number at which amplification of the target gene was within the linear range of the reaction. Relative expression levels for each gene of interest were calculated by normalizing the target gene transcript level (Ct) to the respective GAPDH level with the maximum expression values per gene displayed at a 100 per condition as described previously.⁴²

Histological, immunohistochemical, and scanning electron microscopy analyses

Cell-seeded constructs were fixed in 10% neutral-buffered formalin, dehydrated in graded alcohols, and then embedded in paraffin. Sections (5 μ m) were cut and then stained with hematoxylin and eosin (H&E) using routine histological protocols. For immunohistochemical (IHC) analyses, contractile smooth muscle markers such as α -SMA and SM22 α and intestinal epithelial markers including brush border enzymes, lactase, and maltase were detected using the following primary antibodies: anti- α -SMA (Sigma-Aldrich, St. Louis, MO; 1:200 dilution), anti-SM22 α (Abcam, Cambridge, MA; 1:200 dilution), anti-lactase (Abcam; 1:200 dilution), and anti-maltase (Santa Cruz Biotechnology, Dallas, TX; 1:200 dilution). Sections were then incubated with species-matched Cy3-conjugated secondary antibodies (EMD Millipore, Billerica, MA) and nuclei were counterstained with 4',6-diamidino-2-phenylindole (DAPI). Specimens were visualized using an Axioplan-2 microscope (Carl Zeiss MicroImaging, Thornwood, NY), and representative images were acquired using Axiovision software (version 4.8). In some cases, cell distribution in seeded constructs was determined by scanning electron microscopy (SEM) using previously published procedures.⁴⁴

Statistical analyses

All quantitative measurements were collected with N=3–4 independent replicates per data point from one representative experiment and expressed as mean \pm standard deviation. Data for these measurements were analyzed with the Mann–Whitney U test for independent samples and the Wilcoxon signed-rank test for paired samples using SPSS Statistics software v19.0 (<http://www.spss.com>). Statistically significant values were defined as $p < 0.05$.

Results and discussion

Bi-layer SF and SIS matrices were assessed for their ability to mediate attachment and proliferation of GI SMC lines (Figure 1). Following 24 h of cell seeding, AlamarBlue analysis demonstrated that bi-layer SF scaffolds supported significantly higher levels of attachment for all SMC lines

examined in comparison to SIS matrices. At the 7-day timepoint, relative numbers of each SMC population maintained on both bi-layer SF and SIS scaffolds were significantly elevated over their respective 1-day levels—indicative of cell proliferation. Parallel histological evaluations (hematoxylin and eosin (H&E) analysis) at 7 days revealed that each SMC line displayed a spindle-shaped morphology and was organized into multi-cellular layers primarily dispersed along the periphery of both biomaterial surfaces. Overall, these data show that bi-layer SF matrices are capable of promoting GI SMC attachment and proliferation.

Phenotypic modulation of SMC from a proliferative, synthetic state into a quiescent, contractile phenotype is a dynamic, reversible process which plays key roles in tissue homeostasis and response to injury throughout hollow organs.⁴⁵ In order for biomaterial grafts to reconstitute the contractile properties of tissue defects and support peristalsis of the digestive tract, they must serve as permissive substrates for contractile differentiation of synthetic SMC. Following tissue isolation and ex vivo expansion, primary SMC populations are known to dedifferentiate from a contractile to a synthetic phenotype.^{46–47} Serum deprivation in combination with TGF- β 1 treatment has been reported to induce re-acquisition of contractile markers in ex vivo expanded, synthetic SMC derived from vascular⁴⁸ and urogenital tissues.^{42,46} Therefore, we investigated the potential of these differentiation stimuli to elicit similar responses in GI SMC lines cultured on bi-layer SF and SIS matrices (Figure 2). Real-time RT-PCR analysis demonstrated that following TGF- β 1 treatment, each SMC type cultured on both scaffold groups significantly upregulated α -SMA and SM22 α mRNA transcript levels over respective control values. In addition, IHC evaluations revealed that all TGF- β 1-treated constructs displayed prominent degrees of α -SMA and SM22 α protein expression with qualitatively similar levels of positive staining observed across all cell types and matrix configurations examined. In contrast, non-stimulated control groups displayed qualitatively weak and sparse expression of both markers by comparison (data not shown). These results demonstrate that bi-layer SF matrices are efficacious in supporting contractile differentiation of GI SMC lines.

The diverse epithelia of the GI tract serve a number of critical functions such as enzyme secretion, nutrient absorption, as well as participation in innate and adaptive immune responses.⁴⁹ The ability of tissue-engineered constructs to reconstitute the epithelium of GI tissue defects depends on the potential of scaffold configurations to promote host epithelial ingrowth and differentiation. Bi-layer SF and SIS matrices were first evaluated for their capacity to support attachment and proliferation of two GI epithelial cell lines: T84 and eEP (Figure 3). AlamarBlue analysis revealed that following initial cell seeding, both scaffold groups displayed similar levels of relative cell attachment for each cell line studied.

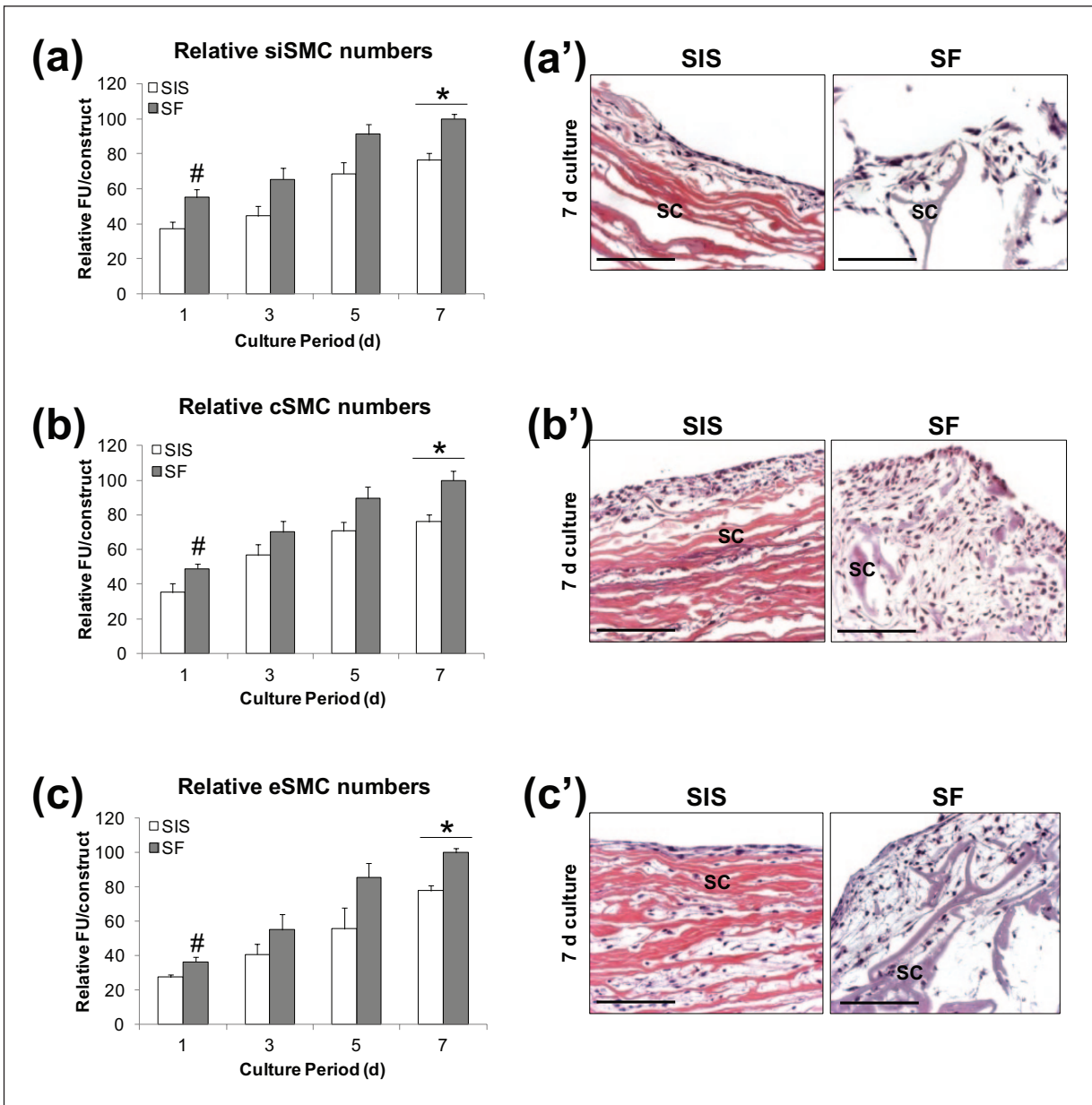


Figure 1. Attachment and proliferation of GI SMC lines on scaffold groups. (a–c) AlamarBlue analysis of the extent of relative cell attachment and proliferation for each SMC line cultured independently on bi-layer SF and SIS matrices over the course of 7 days. FU=Fluorescence units, mean ±SD per data point. #*p*<0.05, in comparison to levels observed on SIS constructs at 1 day of culture. **p*<0.05, in comparison to respective levels observed on SIS and bi-layer SF constructs at 1 day of culture. (a'–c') Photomicrographs of SMC-seeded constructs (H&E-stained sections) following 7 days of culture as described in respective (a–c) counterparts. Scale bars = 200 μm. SC denotes scaffolds. GI: gastrointestinal; SMC: smooth muscle cell; SF: silk fibroin; SIS: small intestinal submucosa; SD: standard deviation; H&E: hematoxylin and eosin.

Following 14 days of culture, significant increases in relative cell numbers were observed in both T84-seeded biomaterials over respective 1-day levels, and histological evaluations (H&E analysis) demonstrated the formation of polarized cell layers lining the perimeter of each scaffold configuration. In addition, relative cell numbers of eEP cells on both bi-layer SF and SIS matrices at 7 days of culture were also found to significantly increase

with respect to 1-day values. However, in contrast to T84 cells, SEM analysis demonstrated that eEP cells were localized in disperse patches along each scaffold surface and did not form detectable cohesive cell layers as observed on other biomaterial substrates.⁵⁰ Our previous results have shown the ability of extracellular matrix coatings such as fibronectin to enhance urologic epithelial interactions to SF biomaterials.⁴² This strategy may

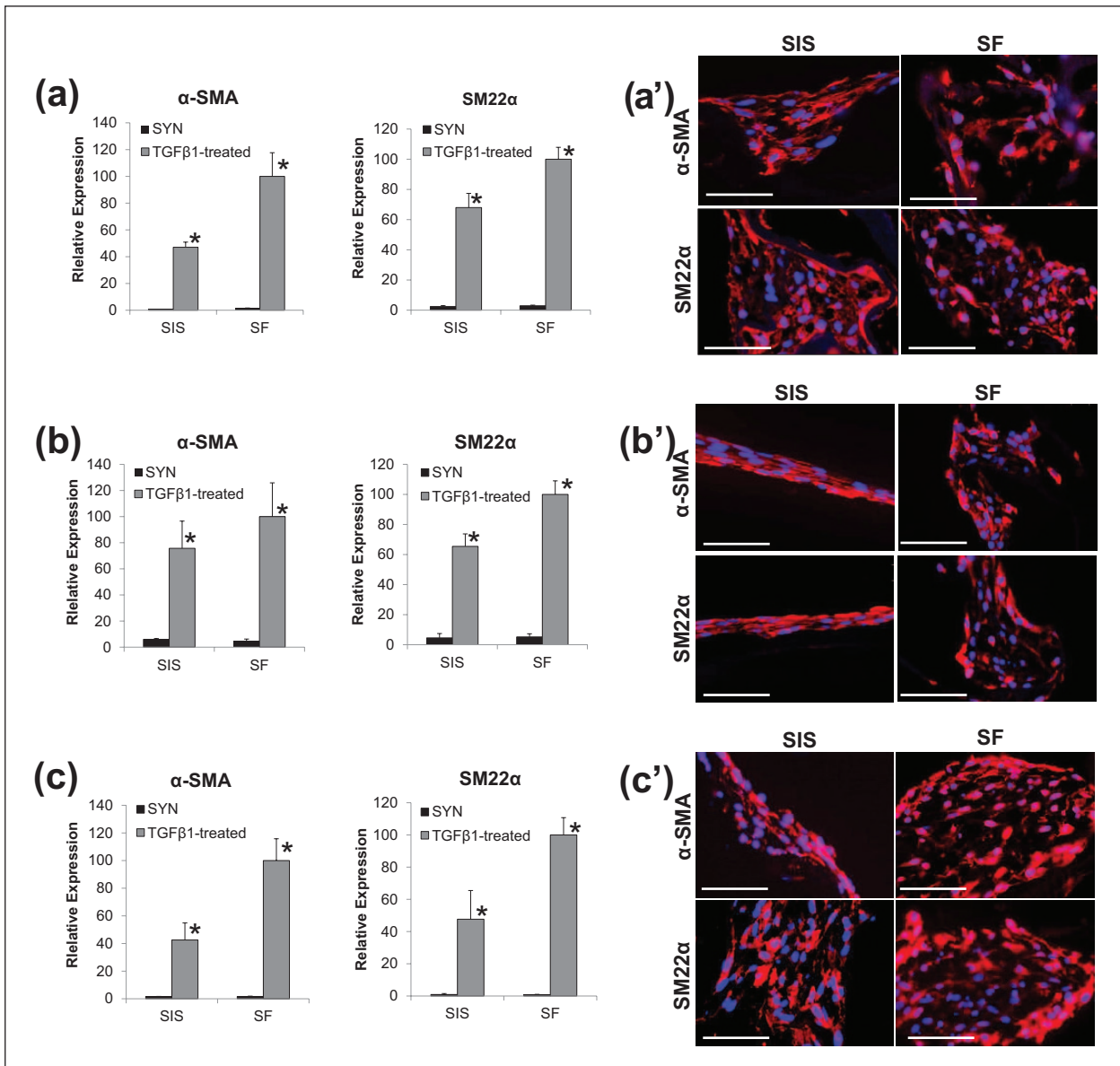


Figure 2. Contractile differentiation of GI SMC lines on matrix groups. (a–c) Real-time RT-PCR analyses of mRNA transcript levels of contractile markers (α -SMA and SM22 α) in synthetic (SYN) and TGF- β 1-treated constructs seeded with SMC lines. Levels normalized to GAPDH expression. Mean \pm SD per data point. For each marker, * $p < 0.05$, in comparison to levels in respective SYN controls. (a'–c') Photomicrographs of contractile protein expression in TGF- β 1-treated constructs as described in respective (a–c) counterparts. Immunofluorescence of contractile proteins (Cy3 fluorophore, red). DAPI nuclear counterstain (blue). Scale bars = 100 μ m.

GI: gastrointestinal; SMC: smooth muscle cell; RT-PCR: reverse transcription polymerase chain reaction; mRNA: messenger RNA; SMA: smooth muscle actin; TGF- β 1: transforming growth factor- β 1; SD: standard deviation; DAPI: 4',6-diamidino-2-phenylindole.

represent a useful approach in order to improve construct cellularity in the current system.

T84 and eEP cell lines have been demonstrated to undergo spontaneous differentiation upon confluency in various two-dimensional (2D) and 3D cell culture models.^{50–53} T84 cells acquire features of small intestinal enterocytes including expression of the brush border enzymes such as lactase and maltase;^{51,52} while proliferating,

CK5+CK14+basal eEP cells mature into a suprabasal cell lineage expressing CK4+CK13+a superficial, squamous cell phenotype which produces involucrin.^{50,53} The bi-layer SF and SIS scaffolds were assessed for their ability to support spontaneous differentiation of T84 and eEP cell lines (Figure 4). Real-time RT-PCR analysis demonstrated that T84 cells cultured on both scaffold groups significantly increased mRNA transcript levels of lactase and maltase at

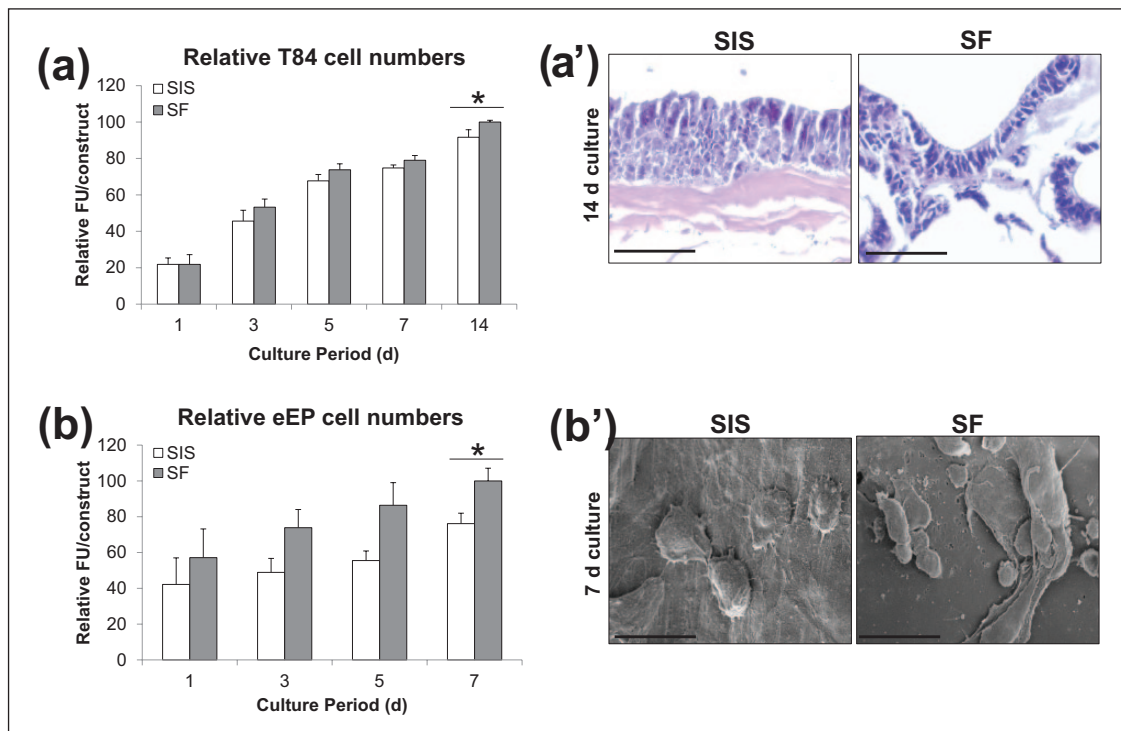


Figure 3. Attachment and proliferation of GI epithelial cell lines on scaffold groups. (a and b) AlamarBlue analysis of the extent of relative cell attachment and proliferation for each epithelial cell line cultured independently on bi-layer SF and SIS matrices over the course of 7 or 14 days. FU = Fluorescence units, mean \pm SD per data point. * $p < 0.05$, in comparison to respective levels observed on SIS and bi-layer SF constructs at 1 day of culture. (a' and b') Photomicrographs of epithelial cell lines cultured on each scaffold group for 7 or 14 days (H&E-stained sections, T84 and SEM, eEP). For a', scale bar = 200 μ m. SC denotes scaffolds. For b', scale bar = 30 μ m.

GI: gastrointestinal; SF: silk fibroin; SIS: small intestinal submucosa; SD: standard deviation; H&E: hematoxylin and eosin; SEM: scanning electron microscopy; eEP: esophageal epithelial.

14 days with respect to 1-day levels. In addition, IHC assessments revealed that T84 cells cultured on each matrix configuration for 14 days displayed qualitatively similar levels of lactase and maltase protein expression. These data show the ability of bi-layer SF scaffolds to support enterocytic differentiation of T84 cells to a comparable degree as SIS.

In contrast to the results obtained with T84 cells, distinct differences were observed in the capacity of the biomaterial groups to promote eEP differentiation. Following 7 days of culture on bi-layer SF scaffolds, real-time RT-PCR analysis demonstrated that eEP cells significantly upregulated CK4 and CK13 mRNA transcript levels over 1-day values, indicative of suprabasal cell specification. However, these markers declined from 1-day baseline levels when eEP cells were cultured on SIS matrices. Evidence for superficial, squamous eEP differentiation was detected in both scaffold groups by the presence of involucrin expression; however, bi-layer SF constructs supported significantly higher mRNA transcript levels (2.4-fold) at 7 days of culture in comparison to SIS matrices. Bioactive growth factors in SIS

scaffolds such as TGF- β 1⁵⁴ have the potential to exert inhibitory roles in eEP cell differentiation processes,⁵⁵ and therefore, their presence may account for the observed differences between the two matrix configurations. Indeed, previous studies have reported incomplete epithelialization of SIS grafts in *in vivo* models of esophageal repair.^{56,57}

Conclusion

The results presented in this study detail the ability of bi-layer SF scaffolds to support attachment, proliferation, and differentiation of human GI epithelial and SMC lines *in vitro*. In comparison to conventional SIS matrices, bi-layer SF scaffolds promoted increased extents of attachment for each SMC line examined as well as a greater propensity for eEP cell differentiation toward suprabasal and superficial phenotypes. Future *in vivo* evaluations in models of defect repair are necessary to determine the potential of these scaffolds for GI organ reconstruction. In summary, bi-layer SF scaffolds represent promising platforms for GI tissue engineering.

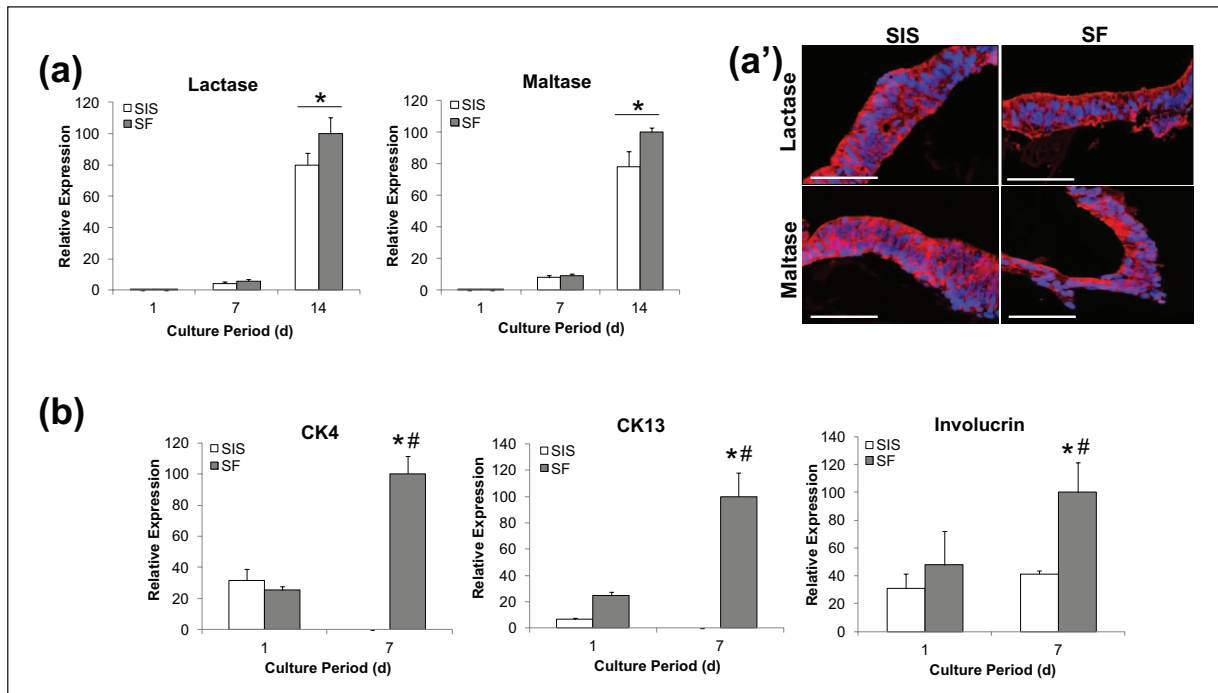


Figure 4. Differentiation of GI epithelial cell lines on matrix groups. Real-time RT-PCR analyses of mRNA transcript levels of (a) enterocyte markers (lactase and maltase) in T84 cells cultured on matrix groups over the course of 14 days and (b) markers of suprabasal (CK4, CK13) and superficial (involucrin) cell phenotypes in eEP cells cultured on scaffold groups over the course of 7 days. * $p < 0.05$, in comparison to respective levels observed on SIS and bi-layer SF constructs at 1 day of culture. # $p < 0.05$, in comparison to respective levels observed in SIS group at 7 days of culture. (a') Photomicrographs of enterocyte protein T84-seeded constructs at 14 days of culture as described in respective (a) counterpart. Immunofluorescence of enterocyte proteins (Cy3 fluorophore, red). DAPI nuclear counterstain (blue). Scale bars = 100 μm. GI: gastrointestinal; RT-PCR: reverse transcription polymerase chain reaction; mRNA: messenger RNA; CK: cytokeratin; eEP: esophageal epithelial; SIS: small intestinal submucosa; SF: silk fibroin; DAPI: 4',6-diamidino-2-phenylindole.

Declaration of conflicting interest

The authors declare that there is no conflict of interests regarding the publication of this article.

Funding

The authors wish to thank the Office of Sponsored Programs at Boston Children's Hospital for pilot study support as well as NIH/NIDDK T32-DK60442 and the Tissue Engineering Resource Center, NIH/NIBIB P41 EB002520.

References

1. Wilmore DW, Byrne TA and Persinger RL. Short bowel syndrome: new therapeutic approaches. *Curr Probl Surg* 1997; 34: 389–444.
2. Frongia G, Kessler M, Weih S, et al. Comparison of LILT and STEP procedures in children with short bowel syndrome—a systematic review of the literature. *J Pediatr Surg* 2013; 48: 1794–1805.
3. Vianna RM, Mangus RS and Tector AJ. Current status of small bowel and multivisceral transplantation. *Adv Surg* 2008; 42: 129–150.
4. Walker SR, Nucci A, Yaworski JA, et al. The Bianchi procedure: a 20-year single institution experience. *J Pediatr Surg* 2006; 41: 113–119.
5. Modi BP, Javid PJ, Jaksic T, et al. First report of the international serial transverse enteroplasty data registry: indications, efficacy, and complications. *J Am Coll Surg* 2007; 204: 365–371.
6. Kumar AR, Li X, Leblanc JF, et al. Proteomic analysis reveals innate immune activity in intestinal transplant dysfunction. *Transplantation* 2011; 92: 112–119.
7. Veenendaal RA, Ringers J and Lamers CB. Clinical aspects of small bowel transplantation. *Scand J Gastroenterol Suppl* 2000; 232: 65–68.
8. Shen KR, Austen WG Jr and Mathisen DJ. Use of a pre-fabricated pectoralis major muscle flap and pedicled jejunal interposition graft for salvage esophageal reconstruction after failed gastric pull-up and colon interposition. *J Thorac Cardiovasc Surg* 2008; 135: 1186–1187.
9. Burgos L, Barrena S, Andrés AM, et al. Colonic interposition for esophageal replacement in children remains a good choice: 33-year median follow-up of 65 patients. *J Pediatr Surg* 2010; 45: 341–345.
10. Bonavina L, Incarbone R, Saino G, et al. Clinical outcome and survival after esophagectomy for carcinoma in elderly patients. *Dis Esophagus* 2003; 16: 90–93.
11. Pedersen RN, Markøw S, Kruse-Andersen S, et al. Esophageal atresia: gastroesophageal functional follow-up in 5–15 year old children. *J Pediatr Surg* 2013; 48: 2487–2495.

12. Deurloo JA, Ekkelkamp S, Hartman EE, et al. Quality of life in adult survivors of correction of esophageal atresia. *Arch Surg* 2005; 140: 976–980.
13. Somppi E, Tammela O, Ruuska T, et al. Outcome of patients operated on for esophageal atresia: 30 years' experience. *J Pediatr Surg* 1998; 33: 1341–1346.
14. Coran AG. A personal experience with 100 consecutive total colectomies and straight ileoanal endorectal pull-throughs for benign disease of the colon and rectum in children and adults. *Ann Surg* 1990; 212: 242–247; discussion 247–248.
15. Pastore RL, Wolff BG and Hodge D. Total abdominal colectomy and ileorectal anastomosis for inflammatory bowel disease. *Dis Colon Rectum* 1997; 40: 1455–1464.
16. Theodoropoulos GE, Papanikolaou IG, Karantanos T, et al. Post-colectomy assessment of gastrointestinal function: a prospective study on colorectal cancer patients. *Tech Coloproctol* 2013; 17: 525–536.
17. Levin DE and Grikscheit TC. Tissue-engineering of the gastrointestinal tract. *Curr Opin Pediatr* 2012; 24: 365–370.
18. Bitar KN, Raghavan S and Zakhem E. Tissue engineering in the gut: developments in neuromusculature. *Gastroenterology* 2014; 146: 1614–1624.
19. Del Gaudio C, Baiguera S, Ajalloueiian F, et al. Are synthetic scaffolds suitable for the development of clinical tissue-engineered tubular organs? *J Biomed Mater Res A* 2014; 102: 2427–2447.
20. Wang ZQ, Watanabe Y and Toki A. Experimental assessment of small intestinal submucosa as a small bowel graft in a rat model. *J Pediatr Surg* 2003; 28: 1596–1601.
21. Demirbilek S, Kanmaz T, Ozardah I, et al. Using porcine small intestinal submucosa in intestinal regeneration. *Pediatr Surg Int* 2003; 19: 588–592.
22. Lopes MF, Cabrita A, Ilharco J, et al. Grafts of porcine intestinal submucosa for repair of cervical and abdominal esophageal defects in the rat. *J Invest Surg* 2006; 19: 105–111.
23. Yamamoto Y, Nakamura T, Shimizu Y, et al. Intrathoracic esophageal replacement with a collagen sponge—silicone double layer tube: evaluation of omental-pedicle wrapping and prolonged placement of an inner stent. *ASAIO J* 2000; 46: 734–739.
24. Chen MK and Badylak SF. Small bowel tissue engineering using small intestinal submucosa as a scaffold. *J Surg Res* 2001; 99: 352–358.
25. Urita Y, Komuro H, Chen G, et al. Regeneration of the esophagus using gastric acellular matrix: an experimental study in a rat model. *Pediatr Surg Int* 2007; 23: 21–26.
26. Lee M, Chang PC and Dunn JC. Evaluation of small intestinal submucosa as scaffolds for intestinal tissue engineering. *J Surg Res* 2008; 147: 168–171.
27. Grikscheit T, Ochoa ER, Srinivasan A, et al. Tissue-engineered esophagus: experimental substitution by onlay patch or interposition. *J Thorac Cardiovasc Surg* 2003; 126: 537–544.
28. Kim SS, Kaihara S, Benvenuto MS, et al. Effects of anastomosis of tissue-engineered neointestine to native small bowel. *J Surg Res* 1999; 87: 6–13.
29. Grikscheit TC, Ochoa ER, Ramsanahie A, et al. Tissue-engineered large intestine resembles native colon with appropriate in vitro physiology and architecture. *Ann Surg* 2003; 238: 35–41.
30. Ceonzo K, Gaynor A, Shaffer L, et al. Polyglycolic acid-induced inflammation: role of hydrolysis and resulting complement activation. *Tissue Eng* 2006; 12: 301–308.
31. Mauney JR, Cannon GM, Lovett ML, et al. Evaluation of gel spun silk-based biomaterials in a murine model of bladder augmentation. *Biomaterials* 2011; 32: 808–818.
32. Warner BW. Tissue engineered small intestine: a viable clinical option? *Ann Surg* 2004; 240: 755–756.
33. Altman GH, Diaz F, Jakuba C, et al. Silk-based biomaterials. *Biomaterials* 2003; 24: 401–416.
34. Kasoju N and Bora U. Silk fibroin in tissue engineering. *Adv Healthc Mater* 2012; 1: 393–412.
35. Wang Y, Rudym DD, Walsh A, et al. In vivo degradation of three-dimensional silk fibroin scaffolds. *Biomaterials* 2008; 29: 3415–3428.
36. Gomez P 3rd, Gil ES, Lovett ML, et al. The effect of manipulation of silk scaffold fabrication parameters on matrix performance in a murine model of bladder augmentation. *Biomaterials* 2011; 32: 7562–7570.
37. Seth A, Chung YG, Gil ES, et al. The performance of silk scaffolds in a rat model of augmentation cystoplasty. *Biomaterials* 2013; 34: 4758–4765.
38. Tu DD, Chung YG, Gil ES, et al. Bladder tissue regeneration using acellular bi-layer silk scaffolds in a large animal model of augmentation cystoplasty. *Biomaterials* 2013; 34: 8681–8689.
39. Chung YG, Algarrahi K, Franck D, et al. The use of bi-layer silk fibroin scaffolds and small intestinal submucosa matrices to support bladder tissue regeneration in a rat model of spinal cord injury. *Biomaterials* 2014; 35: 7452–7459.
40. Chung YG, Tu D, Franck D, et al. Acellular bi-layer silk fibroin scaffolds support tissue regeneration in a rabbit model of onlay urethroplasty. *PLoS One* 2014; 9: e91592.
41. Kim UJ, Park J, Kim HJ, et al. Three-dimensional aqueous-derived biomaterial scaffolds from silk fibroin. *Biomaterials* 2005; 26: 2775–2785.
42. Franck D, Gil ES, Adam RM, et al. Evaluation of silk biomaterials in combination with extracellular matrix coatings for bladder tissue engineering with primary and pluripotent cells. *PLoS One* 2013; 8: e56237.
43. Chomczynski P and Sacchi N. Single-step method of RNA isolation by acid guanidinium thiocyanate-phenol-chloroform extraction. *Anal Biochem* 1987; 162: 156–159.
44. Mauney JR, Blumberg J, Pirun M, et al. Osteogenic differentiation of human bone marrow stromal cells on partially demineralized bone scaffolds in vitro. *Tissue Eng* 2004; 10: 81–92.
45. Beamish JA, He P, Kottke-Marchant K, et al. Molecular regulation of contractile smooth muscle cell phenotype: implications for vascular tissue engineering. *Tissue Eng Part B Rev* 2010; 16: 467–491.
46. Baker SC and Southgate J. Towards control of smooth muscle cell differentiation in synthetic 3D scaffolds. *Biomaterials* 2008; 29: 3357–3366.
47. Kaimoto T, Yasuda O, Ohishi M, et al. Nifedipine inhibits vascular smooth muscle cell dedifferentiation via downregulation of Akt signaling. *Hypertension* 2010; 56: 247–252.
48. Björkerud S. Effects of transforming growth factor-beta 1 on human arterial smooth muscle cells in vitro. *Arterioscler Thromb* 1991; 11: 892–902.

49. Groschwitz KR and Hogan SP. Intestinal barrier function: molecular regulation and disease pathogenesis. *J Allergy Clin Immunol* 2009; 124: 3–20; quiz 21–22.
50. Kalabis J, Wong GS, Vega ME, et al. Isolation and characterization of mouse and human esophageal epithelial cells in 3D organotypic culture. *Nat Protoc* 2012; 7: 235–246.
51. Madara JL, Stafford J, Dharmasathaphorn K, et al. Structural analysis of a human intestinal epithelial cell line. *Gastroenterology* 1987; 92: 1133–1145.
52. Bolte G, Wolburg H, Beuermann K, et al. Specific interaction of food proteins with apical membranes of the human intestinal cell lines Caco-2 and T84. *Clin Chim Acta* 1998; 270: 151–167.
53. Compton CC, Warland G, Nakagawa H, et al. Cellular characterization and successful transfection of serially subcultured normal human esophageal keratinocytes. *J Cell Physiol* 1998; 177: 274–281.
54. McDevitt CA, Wildey GM and Cutrone RM. Transforming growth factor-beta1 in a sterilized tissue derived from the pig small intestine submucosa. *J Biomed Mater Res A* 2003; 67: 637–640.
55. Wang M, Hada M, Huff J, et al. Heavy ions can enhance TGF β mediated epithelial to mesenchymal transition. *J Radiat Res* 2012; 53: 51–57.
56. Badylak S, Meurling S, Chen M, et al. Resorbable bioscaffold for esophageal repair in a dog model. *J Pediatr Surg* 2000; 35: 1097–1103.
57. Tan B, Wang M, Chen X, et al. Tissue engineered esophagus by copper—small intestinal submucosa graft for esophageal repair in a canine model. *Sci China Life Sci* 2014; 57: 248–255.